Observational Study

Medicine®

OPEN

Gemstone spectral imaging in lung cancer

A preliminary study

Yulin Jia, MD[a], Xigang Xiao, PhD[b], Qiulian Sun, BD[b], Huijie Jiang, PhD[c,*]

Abstract

The present study aimed to evaluate the application of gemstone spectral imaging (GSI) for multi-parameter quantitative measurement in lung cancer.

The study retrospectively enrolled 30 patients with lung cancer who underwent chest contrast enhanced CT scan with GSI mode. The GSI viewer was used for image display and data analysis. Optimal energy value, CT values at 40 keV, 70 keV and optimal energy level, spectral curve slope, effective atomic number (Zeff), iodine concentration (IC), and water concentration (WC) at the region of interest were measured and analyzed by statistical methods.

The optimal energy value for optimal contrast-to-noise ratio on plain scan, arterial phase and venous phase was 62.2 ± 5.38 keV, 50.63 ± 3.84 keV, and 52.5 ± 3.7 keV, respectively. There were significant differences in CT values at different energy levels on each scan phase ($P = .033$). The spectral curve slope values among 40 to 70 keV, 40 to 100 keV, and 40 to 140 keV were significantly different ($P < .001$). No significant difference with the slope between arterial phase and venous phase at each energy level interval was observed. Zeff on plain scan, arterial phase, and venous phase was 7.75 ± 0.15, 8.38 ± 0.37, and 8.38 ± 0.30, respectively. Positive correlation was observed among IC, normalized IC, and Zeff on enhanced scan.

Multiparameter of GSI can be used for lung tumor lesion evaluation. Different parameters were correlated and provide multiple qualitative and quantitative information together.

Abbreviations: λ = slope of spectral attenuation curve, CNR = contrast-to-noise ratio, CT = computed tomography, GSI = gemstone spectral imaging, IC = iodine concentration, keV = kiloelectron-volt, kVp = kilovoltage, NIC = normalized iodine concentration, NWC = normalized, PET = positron emission tomography, ROI = region of interest, WC = water concentration, Zeff = effective atomic number.

Keywords: computed tomography, lung cancer, multi-parameter, spectral imaging

1. Introduction

Cancer is one of the leading causes of death worldwide, accounting for 8.2 million deaths in 2012.[1] Lung cancer is the most common cause for 1.59 million deaths, representing about 19.4% of all cancer deaths and was on the rise worldwide.[2] Mortality rates related to cancer can be reduced if the cases are diagnosed and treated early. Screening and early detection are the 2 important efforts for early detection of lung cancer. The most common screening examination used for lung disease is computed tomography (CT). Low dose plain scan is useful for screening and other examinations such as high resolution CT, contrast enhanced CT, positron emission tomography (PET), and so on are used for diagnosing accurately. Besides these, other invasive methods such as thorascopic surgery and transbronchial ultrasound also helps in the definitive diagnosis, but were associated with serious complications. Generally, the routine CT scan for lung mass or nodule was performed by a single energy technique at a certain level of tube voltage, which results in polychromatic data and the imaging technique changed with the advent of spectral CT. Gemstone spectral imaging (GSI), with only one tube and one detector, can produce dual energy because of the fast kilovoltage (kVp)-switching technique.[3] The high and low kVp projections of GSI are mapped onto the material density projections of the selected basis material pair, and a monochromatic energy projection can be synthesized by the weighted sum of the material density projections.[3,4] Thus, the monochromatic images at different energy levels from 40 to 140 keV can be reconstructed, as well as the density images of the two basis materials. Quantitative parameters such as the effective atomic number (Zeff) and the spectral curve can be used for analysis in order to amplify the impalpable differences between different tissues. Several studies have been put forward[5–9] regarding the application of GSI for differentiating the material and identifying the tumor nature. Two studies[8,9] have shown the ability of GSI for differentiating lung cancers from inflammatory masses. However, as far as we know, the effect of multi-parameter quantitative measurement in lung cancer has not been concluded and described in detail.[8,9]

Therefore, the purpose of this study was to investigate the effect of GSI and multi-parameter analysis in quantitative measurement of lung cancer lesion.

Editor: Tobias Sinnberg.

The authors declare no conflicts of interest.

[a] Department of Imaging and Nuclear Medicine, [b] Department of Radiology, the First Affiliated Hospital, [c] Department of Radiology, the Second Affiliated Hospital, Harbin Medical University, Harbin, Heilongjiang, China.

[*] Correspondence: Huijie Jiang, Department of Radiology, the Second Affiliated Hospital, Harbin Medical University, No. 246 Xuefu Road, Nangang District, Harbin, Heilongjiang 150086, China (e-mail: jhjemail@163.com).

Medicine (2018) 97:29(e11170)

Received: 5 December 2017 / Accepted: 25 May 2018

http://dx.doi.org/10.1097/MD.0000000000011170

2. Methods

2.1. Patients

This study was approved by the Ethics Committee of the First Affiliated Hospital of Harbin Medical University, Harbin, China. Written informed consents from all patients were obtained.

One hundred and twenty patients suspected with lung masses and those who underwent clinically indicated chest contrast enhanced CT scan with GSI mode in the Department of Radiology in the First Affiliated Hospital of Harbin Medical University from May to December 2016 were enrolled. Of these, 30 patients with lung cancer as confirmed by pathological evidence through bronchoscopy, transcutaneous puncture biopsy, or surgery after spectral CT scan were included. While a few others in 90 patients, were identified with pneumonia and benign tumor by follow-up. The remaining patients did not receive the final diagnosis and were reviewed on a regular basis. Finally, 30 patients with lung cancer, who had not accepted any antineoplastic treatment before being enrolled, were included in the present analysis.

2.2. CT scan protocol

The examination was performed using a single tube and fast kVp-switching technique between 80 and 140 kVp on a high-definition CT (DiscoveryTM CT 750HD; GE healthcare, Milwaukee, WI). Plain scan and dual-phase contrast-enhanced CT of chest in GSI mode was performed in all the patients. Patients were placed in the craniocaudal direction and examined in the supine position with both arms extended above the head. Plain scan was performed first, and the scan volume ranged from thoracic inlet to base of lung. Then a bolus of 60 to 80 mL nonionic contrast media (Iobitridol 350 mgI/mL, Guerbet, France) was injected into the median cubital vein at a flow rate of 3 mL/s via a high-pressure injector with binocular tube (Ulrich, Germany), followed by 30 mL saline flush. Arterial phase and venous phase were obtained at 25 seconds and 50 seconds after contrast media injection with the same range of plain scan, respectively. The GSI scan parameters were as follows: helical scan mode with 80/140 kVp tube voltage fast switching and 550 mA tube current, 0.8 second tube rotation time, 5 mm slice thickness and interval, 1.25 mm reconstruction interval, and 1.375 pitch.

2.3. Multi-parameter measurement

All monochromatic data were transferred to an advanced workstation (AW 4.5) with GSI Viewer software package (GE Medical Systems, Waukesha, WI) for image analysis and postprocessing. The size of tumor lesion was measured first, which included maximum length, width, and height on 3-dimensional slices. Volume of tumor was calculated by volume = length × width × height/2.[10] The region of interest (ROI) was placed in the relative homogeneous area of the mass or nodule[8] and precautions were taken to avoid necrosis, vessel calcification in it. Meanwhile, the same ROI in the thoracic aorta was determined for background. The optimal energy value for optimal contrast-to-noise ratio (CNR) was obtained first. CT values at 40 kiloelectron-volt (keV), 70 keV and optimal energy level on plain scan and enhanced images were measured. The slope of spectral attenuation curve (λ) was calculated at different energy intervals, including 40 keV to 70 keV, 40 keV to 100 keV, and 40 keV to 140 keV according to the formula, $\lambda_{1-2}=(CT_1\text{-}CT_2)/(keV_2\text{-}keV_1)$. Effective atomic number (Zeff) was obtained on every phase. Iodine and water concentration (IC and WC) of ROIs were measured both in the arterial phase and venous phase (Fig. 1). Then the normalized IC (NIC) and normalized WC (NWC) were calculated ($NIC=IC/IC_{aorta}$, $NWC=WC/WC_{aorta}$). In order to ensure the consistency, the same ROI was placed on different images by copy-and-paste function in one case. All the quantitative parameters were measured and analyzed by 2 independent chest radiologists (each with more than 10 years of experience in thoracic CT diagnosis). Decisions were reached by consensus in cases of discordant interpretations.

2.4. Statistical analysis

All data were presented as mean ± SD. The data were analyzed statistically using SPSS 13.0 (IBM Corporation, Armonk, NY; formerly SPSS Inc., Chicago, IL). The CT values at different energy levels were compared by 1-way analysis of variance and the slopes at different energy sections were compared by paired-samples *t* test. The relationship between Zeff and concentration of iodine and water was analyzed by Pearson product-moment correlation. The larger the Pearson correlation coefficient is, the closer the relationship is. $P<.05$ was considered to indicate a statistically significant difference.

3. Results

Thirty cases met the inclusion criteria and completed CT scans. No complications were observed. The characteristics of the patients and tumors are shown in Table 1.

The average energy values were 62.2 ± 5.38 keV, 50.63 ± 3.84 keV, and 52.5 ± 3.7 keV and provided the best CNR for displaying lung cancer on plain scan, arterial phase, and venous phase, respectively. Both the CT attenuation values of lung lesions and aorta showed a decrease with the increase in photon energy. There were significant differences in CT values of lung cancer at different energy levels on plain scan, arterial phase and venous phase ($F=4.610$, $P=.033$), (Table 2). There was also significant difference between 40 keV and 70 keV ($P=.010$), but no significant difference between 70 keV and optimal keV ($P=.192$). The spectral curve slopes at 40 to 70 keV, 40 to 100 keV, and 40 to 140 keV on each scan phase were significantly different ($P<.001$), but there was no significant difference between the arterial phase and venous phase at these three different energy intervals (Table 3). Zeff on plain scan, arterial phase and venous phase demonstrated values of 7.75 ± 0.15, 8.38 ± 0.37, and 8.38 ± 0.30, respectively. The average values related to IC and WC was listed in Table 4. The relationship between Zeff and concentration of iodine and water were displayed in Figures 2 and 3 based on arterial phase and venous phase, respectively.

4. Discussion

Lung cancer, due to its high risk of death should be diagnosed early and exactly. In this study, spectral CT was applied and multi-parameter information including CT values on different energy levels, spectral curve slopes at different energy intervals, Zeff, and average IC, NIC, WC, and NWC were concluded for lung cancer.

When performing conventional CT, the quantitative indicators included are only size and CT attenuation values on contrast-

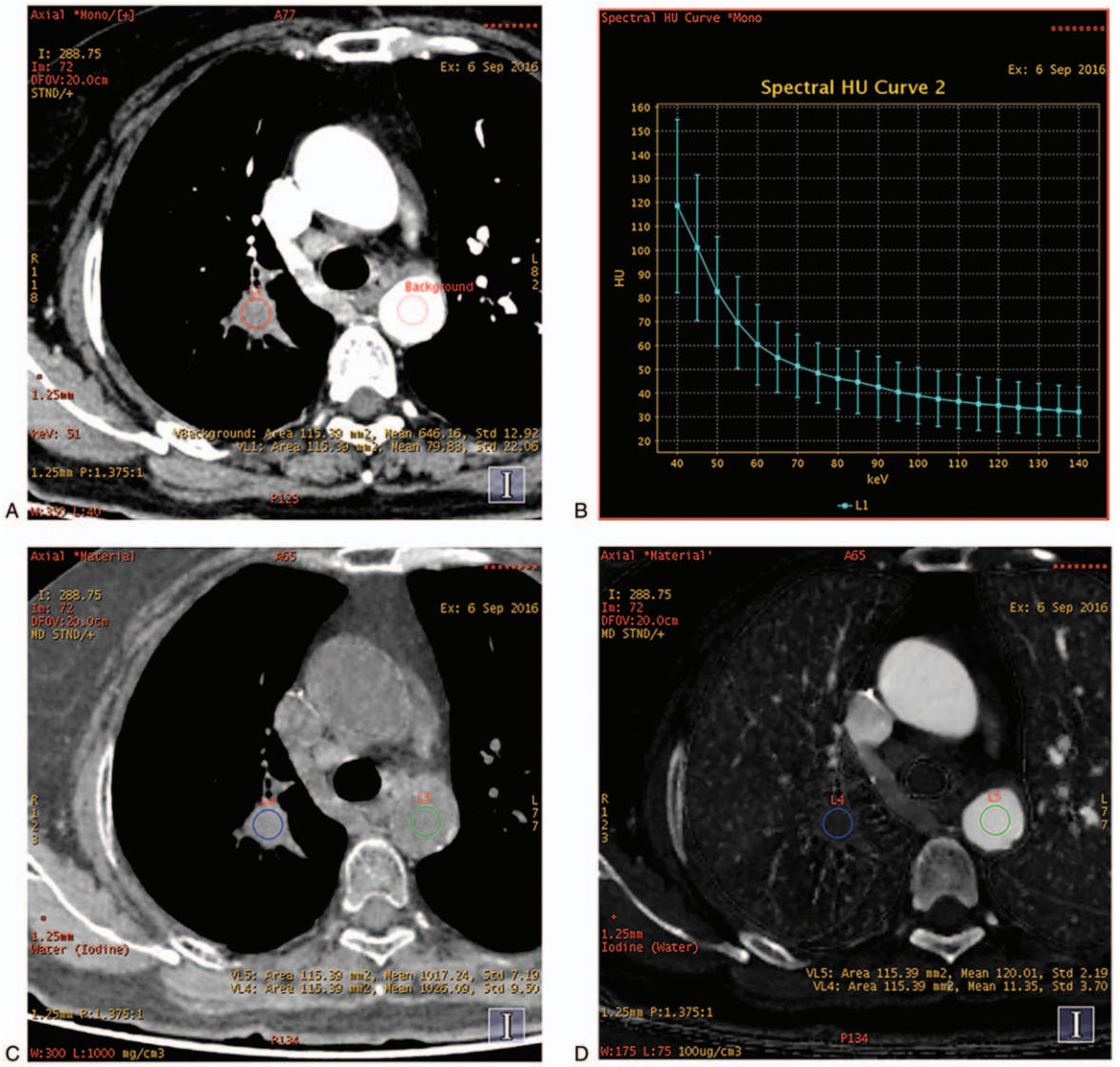

Figure 1. Images of a 71-year-old women with adenocarcinoma in right upper lung lobe. A, monochromatic image at 51 keV (optimal energy level). B, spectral curve (CT values in *y* axis vs keV in *x* axis); C, water concentration image; D, iodine concentration image. CT = computed toography.

Table 1

Patient and tumor characteristics.

Patient characteristics	Number (percentage)
Sex	
Female	12 (40.0)
Male	18 (60.0)
Age, y	59.62±11.34 (34–81)
Position of mass or nodule	
Left upper lobe	4 (13.33)
Left lower lobe	6 (20.0)
Right upper lobe	9 (30.0)
Right middle lobe	0
Right lower lobe	3 (10.0)
Left hilum	8 (26.67)
Right hilum	0
Size	
Length, mm	33.46±15.87
Width, mm	22.44±10.74
Height, mm	26.33±15.09
Volume, mm^3	41.11±19.61
Pathological diagnosis	
Squamous cell carcinoma	6 (20.0)
Adenocarcinoma	10 (33.33)
Small cell carcinoma	13 (43.33)
Large cell neuroendocrine carcinoma	1 (3.33)

enhanced images. Although there are a few advantages with conventional CT, accurate diagnosis is still limited.[11,12] Generally, the morphological changes were considered to be more useful.[13] In this study, spectral imaging with multi-parameter measurement supplies more quantitative information, which can retrieve the shortages of conventional CT. Initially, the optimal energy levels with best CNR were acquired on different scan phases. Monochromatic images with a range of 40–140 keV energy levels can be derived from GSI. But not all the images can be used for observing and diagnosing the lesions as the image quality varies on different energy levels. The most commonly used method to evaluate the image quality is CNR. Therefore, in order to supply the best image quality to display the lesion, the optimal energy level should be chosen accordingly.[14,15] In this study, the average energy value of 62.2±5.38 keV, 50.63±3.84 keV, and 52.5±3.7 keV were found to provide the best CNR for displaying lung cancer on plain scan, arterial phase and venous phase, respectively. The different scan phase is, the different optimal energy level is. The reason may be differences in the attenuation between lesion and background on different phases,

Table 2

CT values at different energy levels.

Scan phase	Plain scan	AP	VP	D_{AP-P}	D_{VP-P}
40 keV	58.92 ± 19.70	144.94 ± 57.15	141.59 ± 46.84	86.01 ± 47.86	82.66 ± 40.64
70 keV	41.70 ± 9.84	69.29 ± 22.78	66.33 ± 20.12	27.59 ± 19.66	23.31 ± 19.01
optimal keV	43.44 ± 11.70	104.33 ± 39.35	96.66 ± 34.43	60.89 ± 35.59	53.23 ± 32.85

F value was 4.610 (P=.033) between different energy levels. P value was .010 and .192 for differences between 40keV and 70 keV, and 70 keV and optimal keV, respectively.
AP = arterial phase, VP = venous phase, D_{AP-P} = difference between arterial phase and plain scan, D_{VP-P} = difference between venous phase and plain scan.

Table 3

Spectral curve slopes at different energy intervals.

Scan phase	Plain scan	Arterial phase	Venous phase	P
40–70 keV	0.57 ± 0.42	2.52 ± 1.26	2.51 ± 1.02	0.936*
40–100 keV	0.32 ± 0.26	1.55 ± 0.78	1.54 ± 0.63	0.866†
40–140 keV	0.21 ± 0.17	1.01 ± 0.50	1.00 ± 0.41	0.880‡

P = .936*, comparison between arterial phase and venous phase of 40–70 keV; 0.866†, comparison between arterial phase and venous phase of 40–100 keV; 0.880‡, comparison between arterial phase and venous phase of 40–140 keV. P value was less than .001 for differences of spectral curve slope at different energy intervals on each scan phase.

Table 4

Average CT values and values related with IC and WC.

Scan phase	IC	WC	NIC	NWC
AP	13.14 ± 6.54	1036.85 ± 14.68	0.12 ± 0.06	1.01 ± 0.01
VP	13.02 ± 5.32	1033.97 ± 14.91	0.30 ± 0.11	1.00 ± 0.01
D_{AP-VP}	0.12 ± 4.55	2.86 ± 15.41	−0.18 ± 0.08	0.01 ± 0.02

IC = iodine concentration, WC = water concentration, NIC = normalized iodine concentration, NWC = normalized water concentration, AP = arterial phase, VP = venous phase, D_{AP-VP} = difference between arterial phase and venous phase.

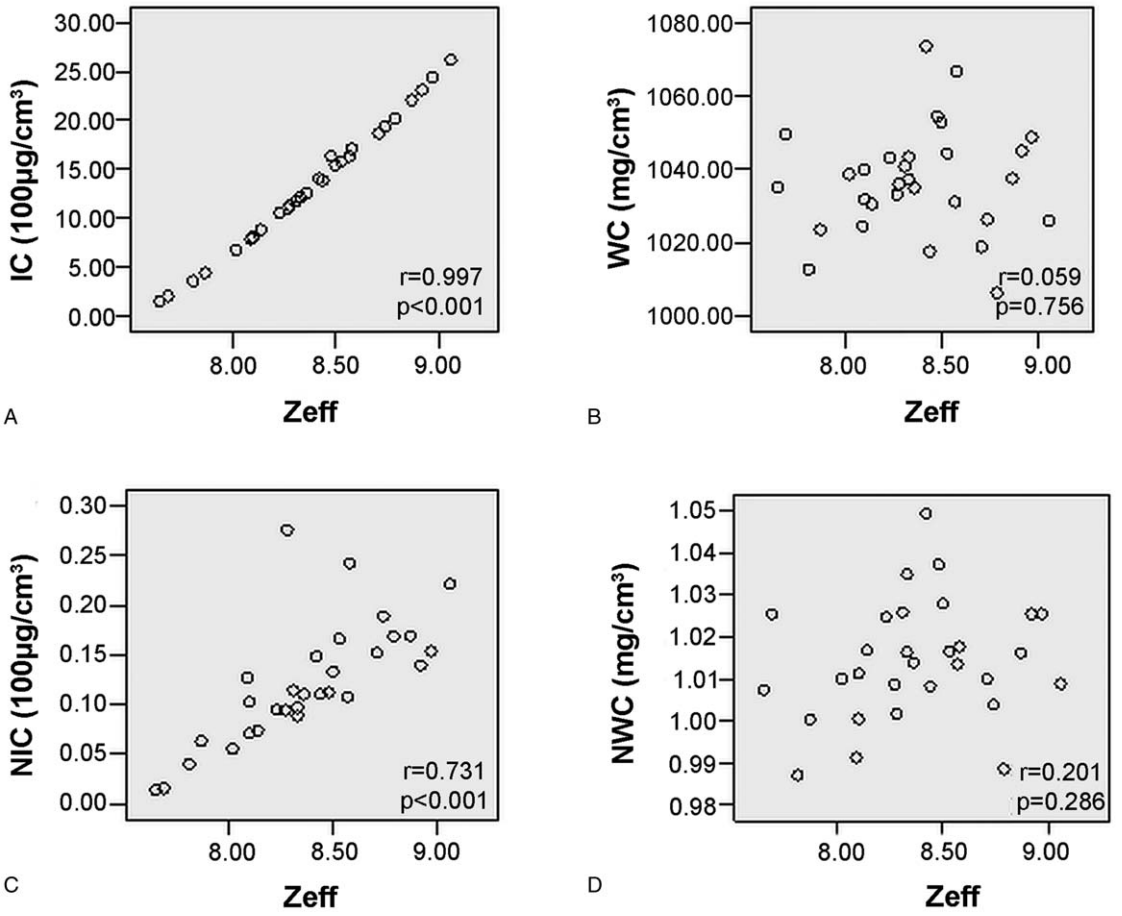

Figure 2. The relationship between effective atomic number (Zeff) and concentration of iodine and water on arterial phase. The scattered graphs demonstrate correlation between Zeff and IC (A), WC (B), NIC (C), and NWC (D). IC = iodine concentration, NIC = normalized iodine concentration, NWC = normalized water concentration, WC = water concentration.

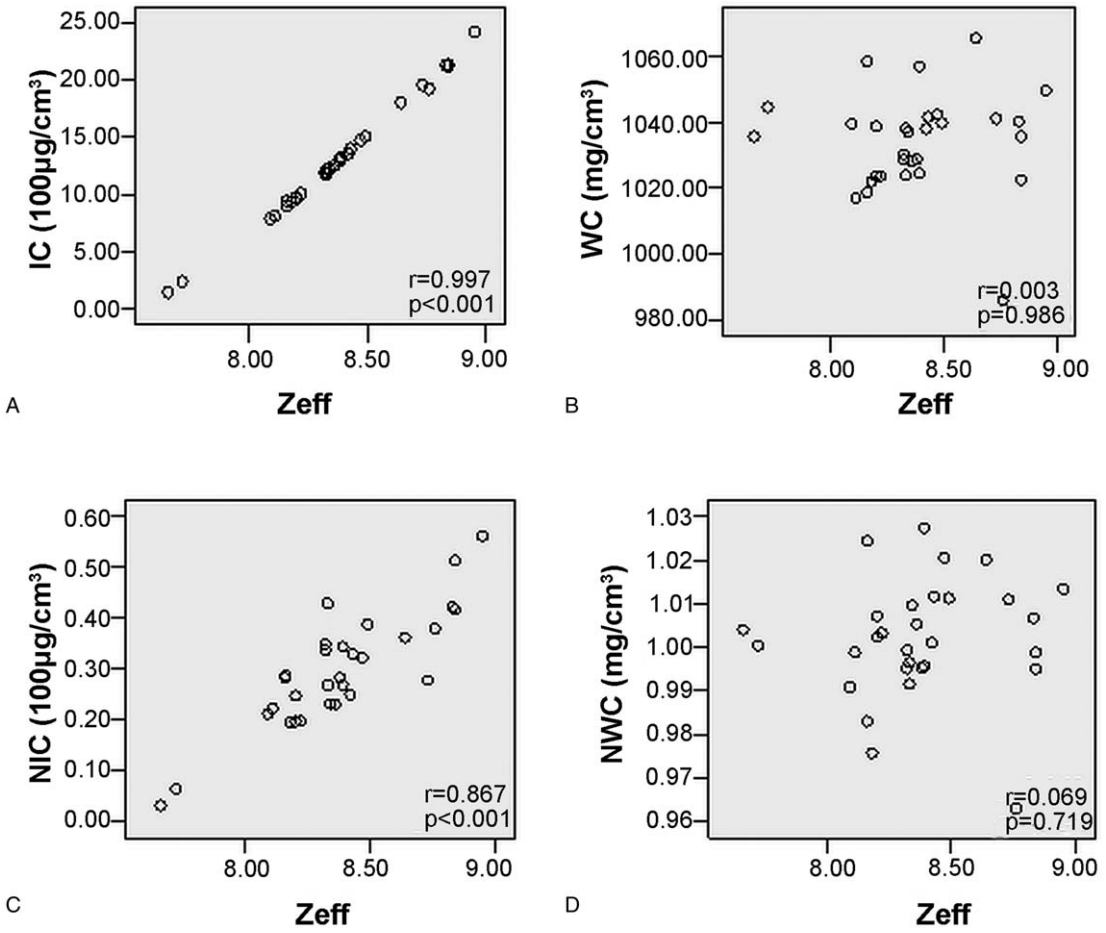

Figure 3. The relationship between effective atomic number (Zeff) and concentration of iodine and water on venous phase. The scattered graphs demonstrate the relationship between Zeff and IC (A), WC (B), NIC (C), NWC (D). IC = iodine concentration, NIC = normalized iodine concentration, NWC = normalized water concentration, WC = water concentration.

that is, the contrast degree between lesion and background changes based on different phases. Hou et al[16] also concluded that optimal monochromatic energy level was required to improve the image quality for lung cancer, but unfortunately the study did not described it in detail. But, the image quality of monochromatic image at optimal energy level was better than that of the polychromatic image derived from conventional CT. The monochromatic image displayed the lesion more clearly, especially in the aspect of morphological changes.

Secondly, CT values on different energy levels were measured. On conventional CT, x-ray photons were generated by only 1 x-ray tube voltage setting, through which a single measurement of density was taken to represent a material. At times, 2 different material compounds may have identical densities, which might be impossible to differentiate such materials by conventional CT. However, it is different on dual energy CT. Years ago, Brooks[17] proposed that x-ray attenuation depended on the energy and the energy dependence might be used to obtain information on chemical composition, which in turn aids in differential diagnosis. Compared with polychromatic x-ray beam on conventional CT, which causes beam hardening and x-ray scatter, the photoelectric effect and Compton scatter collectively existed in the diagnostic energy range. In the low-energy range, the predominant way of interaction between x-ray and matter is photoelectric effect, but in the high-energy range, the Compton scatter is dominant. Using dual energy or spectral CT, 2 projection measurements are acquired and unique material can be characterized better, thus, 2 different materials can be distinguished more uniquely and reliably.[4] In recent years, some studies[14,15,18] showed that CT attenuation values of different lesions decreased as the photon energy increased, which was also concluded for lung cancer results in this study. Meanwhile, we compared CT values on different energy levels. The aim was to make an accurate measurement for the lesion. We tried to find the relative accurate energy level on which CT values are also relatively accurate. In some studies,[8,9] 40 keV and 70 keV were used for measuring CT values, respectively. Actually, CT values at 40 keV are almost the highest values owing to greater attenuation at lower energy levels. So at times, the true CT value may be amplified at 40 keV and might be incorrect. Therefore, we deemed that CT values on 70 keV or optimal energy level are relatively accurate for measurement. Although no significant difference was observed with the regards to the CT values between these two energy levels, as shown by this study, the latter demonstrated higher because of the lower optimal energy level than 70 keV. In this study, moreover, some cases demonstrated CT values of solid lung cancer even lower than 0 HU. Hence, we recommended optimal energy level usage for the measurement and diagnosis. At the same time, the slope of spectral attenuation curve was calculated at different energy

intervals. The spectral curve is a reflection of different lesions or tissues that absorb x-rays at different rates. The results showed that the slopes were different at different energy intervals. It was decreased gradually from 40 to 70 keV interval to 40 to 140 keV interval, which meant that the morphology of spectral attenuation curve was different at different energy intervals. In this study, the curve was steep at 40 to 70 keV interval, and flat at 100 to 140 keV interval in every case. Moreover, the slopes of plain scan and contrast enhanced scans are also different, implying relation between the spectral curve and iodine concentration when the contrast media was used. Besides, there was no significant difference of slopes between arterial phase and venous phase.

At last, Zeff on every phase was also acquired in this study. It is another quantitative index for different materials. It is a new concept derived from atomic number. If the x-ray attenuation coefficient of the element is same as that of a compound, then the element's atomic number is Zeff of the material.[19] Based on this definition, it can be used to identify material composition, especially in the materials with similar densities and same CT attenuation values. Goodsitt et al[19] concluded that Zeff values when computed with dual-energy CT were reasonably accurate. They also proposed that the synthesized monochromatic CT numbers could be very inaccurate, especially for dense tissues that mimic the materials at low energy levels. Several other studies[20,21] showed that Zeff can describe tissue characterization and is useful for differentiating materials. In this study, Zeff values between plain scan and contrast enhanced scan were different. The latter demonstrated much higher values. Also, a clear positive correlation between IC, NIC, and Zeff in both arterial phase and venous phase were found. All these findings suggested that Zeff was more useful for quantitative evaluation of materials. Moreover, average IC, NIC, WC, and NWC of lung cancer were concluded. As we all know, lung cancer cells are highly aggressive, easily invade the corresponding artery and make abundant blood supply diffuse into the extravascular space. The iodine concentration can reflect the blood supply information in the lesion[22] and the water concentration can reflect the water content in both intracellular and extracellular tissues. Some studies[6–9] revealed that IC can be used for differentiating lesions and diseases. Moreover, some other studies[23–25] showed that iodine-enhanced images had a higher sensitivity and accuracy than the degree of contrast enhancement. In other words, IC value is more accurate than CT value in evaluating the blood supply for lesions. Hou e al[9] concluded that 0.34 was the threshold value of NIC for differentiating lung masses, and the sensitivity and specificity were 86% and 100%, respectively. It is a pity that the thresholds of IC and NIC were not concluded in this study, and will be obtained in our future research.

There are also some limitations of this study, which needs further research. First, the sample size was small. There is no control group for comparison to lung cancer, but the contents could satisfy the purpose of this study. More cases should be collected and grouped by some characteristics such as size, pathological type, locations, and so on. Second, not all the correlations between CT values, spectral curve slope, Zeff and IC related values were concluded. Further discussion is required in future studies.

5. Conclusion

In conclusion, CT spectral imaging can derive multiple parameters. Different parameters of GSI are concluded for describing and diagnosing lung cancer by providing multiple qualitative and quantitative information.

Acknowledgements

The authors would like to thank all RTs for patient scanning and RNs for patient preparation. This work was supported by the National Natural Science Foundation of China (Nos. 81471736 and 81671760), the National Science and Technology Pillar Program during the Twelfth 5-Year Plan Period (No. 2015BAI01B09), and Project of Research Foundation of the Talent of Scientific and Technical Innovation of Harbin City (No. 2016RAXYJ063).

Author contributions

Conceptualization: Yulin Jia.
Data curation: Yulin Jia, Xigang Xiao, Qiulian Sun, Huijie Jiang.
Formal analysis: Yulin Jia, Xigang Xiao, Qiulian Sun.
Investigation: Qiulian Sun, Huijie Jiang.
Methodology: Huijie Jiang.
Project administration: Yulin Jia.
Resources: Xigang Xiao, Qiulian Sun.
Software: Xigang Xiao.
Validation: Huijie Jiang.
Visualization: Qiulian Sun.
Writing – original draft: Yulin Jia, Huijie Jiang.
Writing – review & editing: Xigang Xiao, Qiulian Sun.

References

[1] World Cancer Report 2014Geneva, Switzerland: World Health Organization, International Agency for Research on Cancer, WHO Press, 2015. Adv Nutr 2016;7:418–9.
[2] World Health Organization (2012) Cancer, Fact sheet NO.297. Available at: http://www.who.int/mediacentre/factsheets/fs297/en/index.html. Accessed on February 2015. 2012.
[3] Zhang D, Li X, Liu B. Objective characterization of GE discovery CT750 HD scanner: gemstone spectral imaging mode. Med Phys 2011;38:1178–88.
[4] Hawkes DJ, Jackson DF, Parker RP. Tissue analysis by dual-energy computed tomography. Br J Radiol 1986;59:537–42.
[5] Johnson TR, Krauss B, Sedlmair M, et al. Material differentiation by dual energy CT: initial experience. Eur Radiol 2007;17:1510–7.
[6] Li X, Zhao R, Liu B, et al. Gemstone spectral imaging dual-energy computed tomography: a novel technique to determine urinary stone composition. Urology 2013;81:727–30.
[7] Lee SH, Hur J, Kim YJ, et al. Additional value of dual-energy CT to differentiate between benign and malignant mediastinal tumors: an initial experience. Eur J Radiol 2013;82:2043–9.
[8] Wang G, Zhang C, Li M, et al. Preliminary application of high-definition computed tomographic Gemstone Spectral Imaging in lung cancer. J Comput Assist Tomogr 2014;38:77–81.
[9] Hou WS, Wu HW, Yin Y, et al. Differentiation of lung cancers from inflammatory masses with dual-energy spectral CT imaging. Acad Radiol 2015;22:337–44.
[10] Naito S, von Eschenbach AC, Giavazzi R, et al. Growth and metastasis of tumor cells isolated from a human renal cell carcinoma implanted into different organs of nude mice. Cancer Res 1986;46:4109–15.
[11] Goodsitt MM, Chan HP, Way TW, et al. Accuracy of the CT numbers of simulated lung nodules imaged with multi-detector CT scanners. Med Phys 2006;33:3006–17.
[12] Goodsitt MM, Chan HP, Way TW, et al. Quantitative CT of lung nodules: dependence of calibration on patient body size, anatomic region, and calibration nodule size for single- and dual-energy techniques. Med Phys 2009;36:3107–21.
[13] Warth A. Diagnosis, prognosis, and prediction of non-small cell lung cancer. Importance of morphology, immunohistochemistry and molecular pathology. Pathologe 2015;36(Suppl 2):194–200.
[14] Zhao LQ, He W, Li JY, et al. Improving image quality in portal venography with spectral CT imaging. Eur J Radiol 2012;81:1677–81.

[15] Jia Y, Zhang J, Fan J, et al. Gemstone spectral imaging reduced artefacts from metal coils or clips after treatment of cerebral aneurysms: a retrospective study of 35 patients. Br J Radiol 2015;88:20150222.
[16] Hou W, Sun X, Yin Y, et al. Improving image quality for lung cancer imaging with optimal monochromatic energy level in dual energy spectral computed tomography. J Comput Assist Tomogr 2016;40:243–7.
[17] Brooks RA. A quantitative theory of the Hounsfield unit and its application to dual energy scanning. J Comput Assist Tomogr 1977; 1:487–93.
[18] Matsumoto K, Jinzaki M, Tanami Y, et al. Virtual monochromatic spectral imaging with fast kilovoltage switching: improved image quality as compared with that obtained with conventional 120-kVp CT. Radiology 2011;259:257–62.
[19] Goodsitt MM, Christodoulou EG, Larson SC. Accuracies of the synthesized monochromatic CT numbers and effective atomic numbers obtained with a rapid kVp switching dual energy CT scanner. Med Phys 2011;38:2222–32.
[20] Gonzalez-Perez V, Arana E, Barrios M, et al. Differentiation of benign and malignant lung lesions: dual-energy computed tomography findings. Eur J Radiol 2016;85:1765–72.
[21] Ju Y, Liu A, Dong Y, et al. The value of nonenhanced single-source dual-energy CT for differentiating metastases from adenoma in adrenal glands. Acad Radiol 2015;22:834–9.
[22] Lv P, Lin XZ, Li J, et al. Differentiation of small hepatic hemangioma from small hepatocellular carcinoma: recently introduced spectral CT method. Radiology 2011;259:720–9.
[23] Swensen SJ, Brown LR, Colby TV, et al. Pulmonary nodules: CT evaluation of enhancement with iodinated contrast material. Radiology 1995;194:393–8.
[24] Yamashita K, Matsunobe S, Tsuda T, et al. Solitary pulmonary nodule: preliminary study of evaluation with incremental dynamic CT. Radiology 1995;194:399–405.
[25] Swensen SJ, Viggiano RW, Midthun DE, et al. Lung nodule enhancement at CT: multicenter study. Radiology 2000;214:73–80.